Ileocolonic Healing After Extended Small Bowel Resection in Mice: NOD2 Deficiency Impairs Anastomotic Healing and Postoperative Outcome

Maria Witte, MD,[*] *Johannes Reiner, MD,*[†] *Karen Bannert, PhD,*[†] *Robert Jaster, MD,*[†] *Christian Maschmeier, MSc,*[†] *Clemens Schafmayer, MD,*[*] *Georg Lamprecht, MD,*[†] *and Peggy Berlin, PhD*[†]

Background: Nucleotide-binding oligomerization domain-containing protein 2 (*NOD2*) mutations are a genetic risk factor for Crohn disease. Ileocecal resection is the most often performed surgery in Crohn disease. We investigated the effect of *Nod2* knockout (KO) status on anastomotic healing after extended ileocecal resection (ICR) in mice.

Methods: Male C57BL6/J wild-type and *Nod2* KO mice underwent an 11 cm resection of the terminal ileum including the cecum. An end-to-end jejuno-colostomy was performed. Animals were killed after 5 days investigating bursting pressure, hydroxyproline content, and expression of matrix metabolism genes, key cytokines, and histology of the anastomosis.

Results: Mortality was higher in the *Nod2* KO group but not because of local or septic complications. Bursting pressure was significantly reduced in the *Nod2* KO mice (32.5 vs 78.0 mmHg, $P < 0.0024$), whereas hydroxyprolin content was equal. The amount of granulation tissue at the anastomosis was similar but more unstructured in the *Nod2* KO mice. Gene expression measured by real-time polymerase chain reaction showed significantly increased expression for Collagen 1alpha and for collagen degradation as measured by matrix metalloproteinase-2, -9, and -13 in the *Nod2* KO mice. Gelatinase activity from anastomotic tissue was enhanced by *Nod2* status. Gene expression of arginase I, tumor necrosis factor-α, and transforming growth factor-ß but not inducible nitric oxide synthase were also increased at the anastomosis in the *Nod2* KO mice compared with the control mice.

Conclusions: We found that *Nod2* deficiency results in significantly reduced bursting pressure after ileocecal resection. This effect is mediated via an increased matrix turnover. Patients with genetic *NOD2* variations may be prone to anastomotic failure after bowel resection.

Key Words: *NOD2*, anastomosis, surgery, healing, ileocecal, Crohn disease, short bowel

INTRODUCTION

Wound healing is a well-orchestrated cascade of cellular and immunological steps ideally leading to primary closure of the defect without qualitative restriction. Failure of wound healing in the gastrointestinal tract has significant clinical consequences such as sepsis, reoperation, stoma formation, or death. Most patients with Crohn disease (CD) have to undergo surgery at least once in their life.[1] Ileocecal resection (ICR) is one of the most frequently performed surgical operations in patients with CD, necessitating an ileocolonic anastomosis.

Whether patients with CD have impaired intestinal wound healing per se or whether it is attributed to their specific medication or other factors is unclear. Medication for CD modulates the immune system, but recent studies have failed to show a detrimental effect of biologic medication on anastomotic healing in experimental models[2, 3] and after ileocecal resection in humans.[4]

So far, the pathophysiology of CD has not been fully understood, but patients with certain mutations in the nucleotide-binding oligomerization domain-containing protein 2 (*NOD2*) have an up to 17-fold increased risk of developing CD.[5, 6] It is estimated that homozygous or heterozygous *NOD2* mutations are prevalent in up to 40% of patients with chronic inflammatory bowel disease.[7, 8] Research has shown that NOD2 is an intracellular sensor for bacterial peptidoglycan, leading to an activation of the nuclear factor-kappa B (NF-κB) cascade via muramyl dipeptide (MDP).[9] It is present in many cell types such as myeloid, lymphoid, and decidual stromal cells but is predominant in the Paneth cells of the terminal ileum,[5] where the secretion of defensins is activated via NOD2.[9]

Received for publications September 13, 2020; Editorial Decision January 1, 2021.

From the *Department of General, Visceral, Vascular and Transplant Surgery, Rostock University Medical Center, Rostock, Germany; †Division of Gastroenterology and Endocrinology, Department of Medicine II, Rostock University Medical Center, Rostock, Germany

Supported by: This work was supported by a grant from the Deutsche Forschungsgemeinschaft (BE 6292/1-1 to PB).

Address correspondence to: Maria Witte, MD, Department of General, Visceral, Vascular and Transplant Surgery, Rostock University Medical Center, Schillingallee 35, 18057 Rostock, Germany (maria.witte@med.uni-rostock.de).

doi: 10.1093/ibd/izab022
Published online 8 February 2021

Patients with CD and *NOD2* mutations have impaired clinical outcome as indicated by earlier surgery[10, 11] and less response to antibiotic treatment in regard to fistula healing.[12] Furthermore, patients with *NOD2* mutations have worse clinical outcome in sepsis[13] and a higher risk of developing intestinal failure independent of CD.[14]

Previous work in cutaneous wound healing has shown that *Nod2*-deficient mice display delayed excisional healing because of delayed re-epithelialization and altered inflammation.[15] Stimulation of the NOD2 cascade with external muramyl dipeptide (MDP), however, does not restore impaired excisional healing[16] but alters the inflammatory response and delays it further.[17]

A previous study established a resectional bowel model in mice,[18] allowing an examination of the role of NOD2 after resection of 40% of the small bowel including the cecum and performing an end-to-end jejuno-colostomy. Here, we show the results of this extensive small bowel resection on anastomotic healing in wild-type (WT) and *Nod2*-deficient mice (*Nod2* KO). This study is the first to show the negative effect of *Nod2* deficiency on anastomotic healing .

MATERIALS AND METHODS

Mouse Monitoring

All mouse experiments were performed according to the EU Directive 2010/63/EU of the animal protection law and were approved by the local animal committee (Landesamt für Landwirtschaft, Lebensmittelsicherheit und Fischerei, Mecklenburg-Vorpommern, 722.3-1.1-002/13).

Mouse breeding and housing were performed per previously published work.[19] Briefly, male C57Bl6/J mice and B6.129S1-*Nod2*^{tm1Flv}/J mice were purchased from Jackson Laboratory (Bar Harbor, ME) and bred in the animal facilities at the Institute for Experimental Surgery, University Medical Center Rostock (Rostock, Germany). Animals were allowed to acclimatize and had free access to chow and water. Two days before surgery, the mice were switched to a liquid diet (AIN 93G, Sniff, Soest, Germany) and kept on this diet until the end of the experiment. The mice were weighed and monitored for a wellness score daily each morning.[20] If the mice had a wellness score <4 or lost more than 30% of their initial weight, they were euthanized and autopsied. Stool consistency was categorized daily (3 = normal, 2 = normal-soft, 1 = soft-diarrhea, 0 = diarrhea).

Operative Procedure

Mice were anesthetized using ketamine/xylazine intraperitoneally, then intubated and ventilated during the procedure. A median laparotomy and eventration of the small bowel and cecum were performed. Eleven centimeters of the small bowel proximal to the cecum and the cecum were resected. Mesenteric vessels were clipped using microclips (Weck, Horizon, Germany). The jejuno-colonic anastomosis was performed with single interrupted stitches using 8-0 monofilament suture material under an operating microscope with 16× magnification. The fascia and skin were closed with a 6-0 prolene suture. Mice were resuscitated with 1 mL sodium chloride 0.9% solution and received 5 mg/kg carprofen as an analgesic, both subcutaneously. They were kept in a warming terrarium for at least 4 hours before returning to the cages.

Bursting Pressure Measurement

A relaparotomy was performed on postoperative day 5, and the anastomosis was visualized without perturbing the adhesions. An infusion catheter was introduced 2 cm proximal to the anastomosis and a transducer catheter was introduced 2 cm distal to the anastomosis. Both segments were then ligated with nylon suture. An infusion pump (Lineomat, VEB MLW, Berlin, Germany) injected saline at 1 mL/min. The increasing pressure was measured continuously, and a sudden drop in pressure and extravasation of fluid from the anastomosis indicated bursting. The maximum pressure before the drop was recorded as the bursting pressure. Animals were euthanized at the end of the measurement by cervical dislocation.

Tissue Harvest

The anastomosis, including bowel segments 1 cm proximal and 1 cm distal, was harvested for analysis. The tissue was longitudinally cut in half and either fixed in 4% formalin or shock-frozen at –80°C for later RNA or protein analysis. Tissue that was used for bursting pressure measurement was not used for RNA isolation.

RNA Isolation

RNA isolation was done using the RNeasy Minikit (Qiagen, Hilden, Germany). Briefly, 30 mg tissue was homogenized using a tissue lyser at 50 Hz for 5 minutes. After centrifugation at 14.000*g* for 3 minutes, the supernatant was mixed with an equal volume of 70% ethanol and then applied on a RNeasy column, following the manufacturer's instructions. A DNA digestion at room temperature was performed using the RNase-free DNase set (Qiagen, Hilden, Germany). The RNA quality was checked by agarose gel electrophoresis, and cDNA synthesis using 2 µg RNA as template was done using a high-capacity cDNA reverse transcription kit (Applied Biosystems, Darmstadt, Germany).

Quantitative Real-Time Polymerase Chain Reaction

Gene expression was analyzed by quantitative real-time polymerase chain reaction (PCR) using the TaqMan Universal PCR Master Mix and the predesigned TaqMan gene expression assays (Supplemental Table 1). We used 15 ng cDNA for PCR reaction. Analyses were performed in triplicate on a ViiA7 sequence detection system (Applied Biosystems). The PCR

conditions were as follows: 95°C for 10 minutes, 55 cycles of 15 seconds at 95°C, 1 minute at 60°C. The data were normalized to the housekeeping gene (*GAPDH*). Expression levels of the genes of interest were given as $2^{-\Delta cT}$.

Protein Isolation and Hydroxyprolin Measurement

Approximately 30 mg tissue from shock-frozen samples was lysed in 300 µl lysis buffer at 50 Hz for 5 minutes. Lysates were cleared by centrifugation (1000*g* for 10 minutes), and the supernatant was saved. Protein concentration was determined using the Bradford assay.

Hydroxyprolin (OHP) was determined using the Hydroxyprolin Assay Kit MAK008 (Sigma-Aldrich, Steinheim, Germany). Briefly, 10 mg tissue from the anastomosis was homogenized with 100 µL distilled water using a tissue lyser for 5 minutes at 50 Hz. Lysate was mixed with 100 µL 37% hydrochloric acid and hydrolyzed at 120°C for 3 hours. Next, 20 µL lysate was added into a 96-well plate. Standard was run in parallel. All samples were run in triplicate following the manufacturer's protocol. Analysis was done using the Glomax Multi Detection System at 560 nm absorption. The OHP content is reported as µg OHP/µg protein.

Zymography

The 10% zymogram-ready gels (Biorad Laboratories GmbH, Munich, Germany) were loaded with 40 µg protein/probe mixed with a zymography buffer. Recombinant mouse matrix metalloproteinase (MMP)-2 and MMP-9 standards (Biolegend Inc., San Diego, CA) were run as controls (5 ng each). Electrophoresis was run at 200V for 1 hour. After sample separation, gels were incubated twice for 30 minutes in a renaturing buffer and then twice in a denaturing buffer (30 minutes and overnight; Biorad Laboratories GmbH). After washing 3 times for 15 minutes in water, gels were stained for 60 minutes in Simply Blue Safe Stain. Finally, excess dye was removed by washing in water. Clear, ie, nonstained areas, indicated MMP-digested zones.

Histology

The excised and formalin-fixed tissue of the anastomosis was further processed to obtain longitudinally oriented tissue samples that were paraffin-embedded and cut into 4 µm sections using an electronic rotary microtome (Microm HM340E, Thermo Scientific). Tissue slices were stained with hematoxylin and eosin. Four technically well-processed tissue sections of the anastomoses were analyzed per group by 6 different individuals in a blinded manner using an Axio Observer inverted microscope (Zeiss) using 10× magnification and Zen 2.3 software.

Immunohistochemical staining of the anastomoses was performed using the avidin-biotin-peroxidase technique (Vector Laboratories, Burlingame, CA). Slides were deparaffinized and rehydrated. Heat-mediated antigen retrieval was performed in citrate buffer (95°C, 20 minutes) using a pressure cooker (Retriever2100, BioVendor, Germany). Sections were incubated for 15 minutes with an Avidin D solution followed by 15 minutes incubation with a biotin solution to block endogenous biotin (Avidin/Biotin blocking kit, Vector Laboratories). Next, slides were incubated for 60 minutes with phosphate-buffered saline (PBS) containing 2% goat serum (Vector Laboratories) followed by exposure to rabbit anti-mouse antibodies against proliferating cell nuclear antigen (PCNA) staining (FL-261, 1:200), arginase isoform I (H-52, 1:200), and nitric oxide synthase 2 (H-174, 1:200; all Santa Cruz Biotechnology, Dallas, TX) diluted in 2% goat serum/PBS for 90 minutes. Negative controls omitted the primary antibody. The slides were washed and subsequently incubated with 1 µg/mL biotinylated goat anti-rabbit immunoglobulin (Vector Laboratories) diluted in 2% goat serum/PBS for 30 minutes. After extensive washing, sections were incubated with the avidin-biotin complex reagent for 30 minutes. The target protein was visualized by peroxidase substrate containing the chromogen NovaRed. Slides were counterstained with hematoxylin and embedded in Pertex (Medite, Germany).

The amount of granulation tissue was quantified by hematoxylin and eosin staining and the cellular proliferation was measured by PCNA staining using a simple scoring system (absence = 0, slight = 1, moderate = 2, and massive = 3) as described by Radulescu et al.[21]

Humane Endpoints

A wellness score <4 points, body weight loss of >30% from the initial weight, and a distended abdomen together with persistent constipation or dehydration combined with massive diarrhea were defined as humane endpoints. Mice that reached ≥1 humane endpoints were killed immediately and underwent autopsy. These mice were included for analysis of the wellness score, weight, and stool consistency but were excluded otherwise.

Statistics

Numerical results were first tested for normality and then analyzed by either the unpaired Student *t* test or the Mann-Whitney *U* test with $P < 0.05$ as a significance level, using GraphPad Prism, Version 8.4.3 (GraphPad Software). Results are displayed as median with interquartile range as indicated in the legends of the figures. Kaplan-Meier curves were created to analyze the survival of the WT and *Nod2* KO mice. Kaplan-Meier curves were compared using the log-rank Cox-Mantel test. Scoring of the histological sections was tested for interobserver variability using the free-marginal multirater kappa.

RESULTS

Survival, Wellness Score, and Weight Course

In the WT ICR group, 16/20 mice reached the planned endpoint. The 5-day survival was 80% for the WT ICR mice. In contrast, only 13/20 *Nod2* KO mice survived until the end of the experiment. The 5-day survival was 61% for *Nod2* KO ICR mice (Fig. 1A; $P = 0.2072$ log-rank test). Reasons for early death were ileus because of adhesions (n = 2), anastomotic stricture (n = 2), insufficiency (n = 2, 1 in each group), or unclear (n = 5). Immediately after the operation, the wellness score dropped from 11 (maximum score) to 7. Thereafter it quickly returned to normal values, indicating a rapid recovery in all the mice that survived to day 5 (Fig. 1B). In both groups, mice lost 17% to 18% body weight postoperatively. Weight loss occurred predominantly during the first 24 hours after the operation and plateaued thereafter (Fig. 1C). Stool consistency was looser in the *Nod2* KO group compared with the WT group at day 1, but this was not significant and normalized after 72 hours (Fig. 1D). Taken together, the data indicated that early clinical postoperative recovery after extensive ICR did not differ between WT and *Nod2* KO mice.

Bursting Pressure, OHP Concentration, and Collagen Metabolism

Anastomotic healing is determined by qualitative and quantitative factors. Surgical skills contribute to qualitative factors. To control for these parameters, all operations were performed by the same surgeon (MW). Bursting pressure measured at day 5 postoperatively represented the balance between the amount and the quality of newly formed matrix at the anastomosis and tissue breakdown. Bursting pressure was significantly lower in the *Nod2* KO group than in the WT group ($P = 0.0024$; Fig. 2). No bowel burst outside the anastomosis.

The OHP concentration was measured as an index of the amount of collagen in the anastomotic tissue. It was not different between both groups (0.026 µg vs 0.032 µg OHP/µg protein). At the mRNA level, collagen 1alpha expression but not collagen 3alpha or fibronectin expression was significantly increased in the *Nod2* KO mice compared with the WT mice (Fig. 3), suggesting that the *Nod2* KO mice had an increased collagen 1 turnover. In line with these results, MMP-2, MMP-9, and MMP-13 mRNA expression was significantly increased in the *Nod2* KO mice, indicating an increased tissue matrix breakdown. Notably, the expression of mRNA for all matrix genes measured was very homogeneous in the WT group but ranged widely in the *Nod2* KO group.

Zymography from anastomotic tissue is shown for 4 representative mice per group in Fig. 4. The predominant MMPs were MMP-2 at 40 kDA and 60 kDa and MMP-9 at 90 kDa molecular weight. Both MMPs had collagen I and fibronectin as the main substrate, which was predominant at the anastomosis

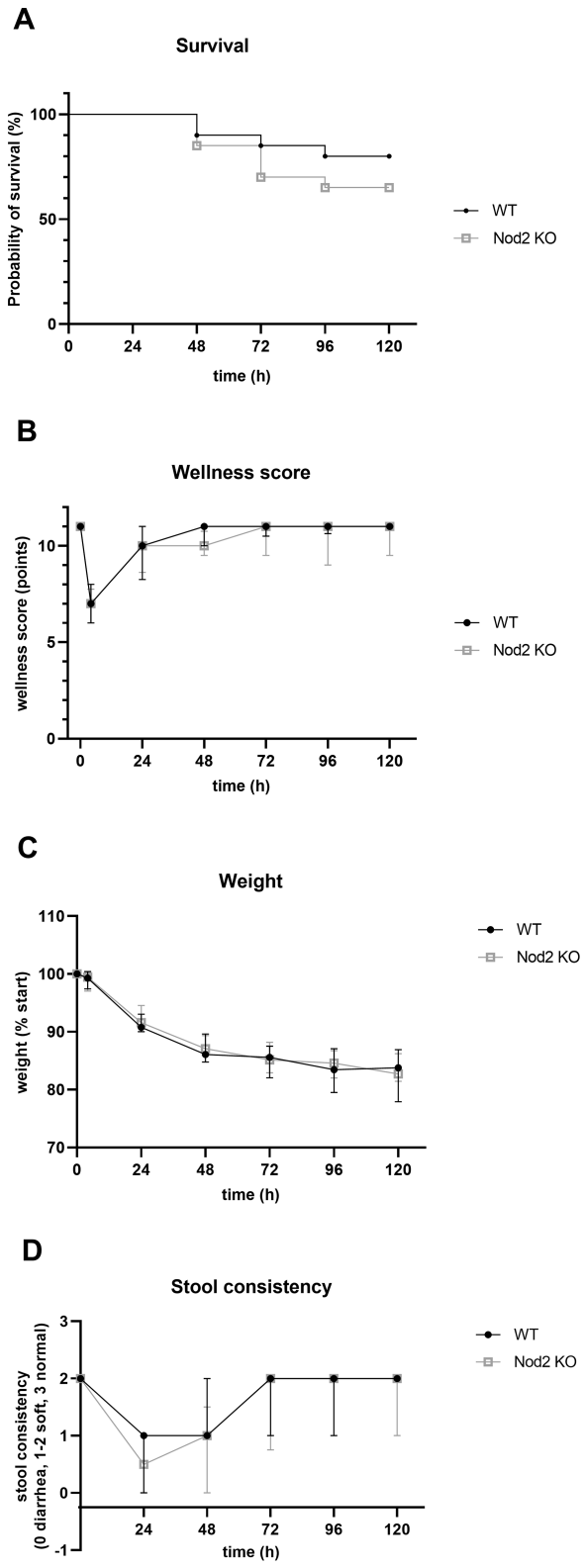

FIGURE 1. A, Kaplan-Meier survival curves of both experimental groups. Four of 20 WT mice and 7 of 20 *Nod2* KO mice reached humane endpoints and were killed before 120 hours ($P = 0.2072$, log-rank test).

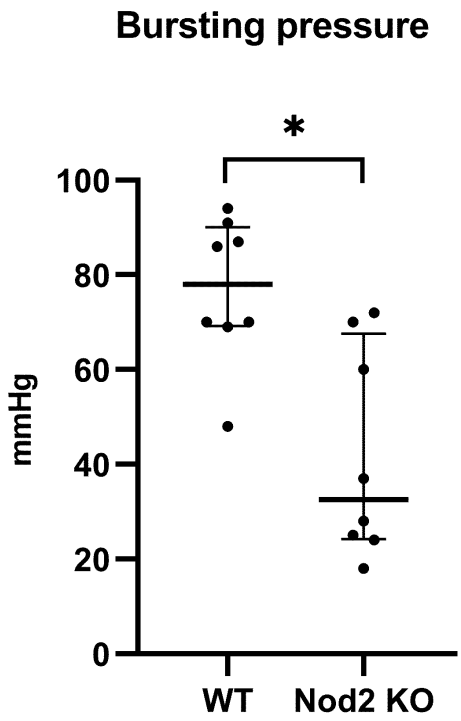

FIGURE 2. Bursting pressure measured at day 5 postoperation showed a significant reduced bursting pressure for the *Nod2* KO mice compared with the WT mice (median [IQR], 32.5 [24.2-67.5] for the *Nod2* KO mice; 78.0 [69.2-90.0] for WT mice; $P < 0.0024$ by unpaired test; n = 8 per group represented by each symbol, displayed as median + IQR in mm Hg). Bursting pressure was measured in situ without removing the adhesions at the anastomosis. IQR indicates the interquartile ratio. *P = 0.0024 WT vs. *Nod2* KO, unpaired *t*-test.

at day 5. Note that the pattern of MMP distribution was similar between the WT and *Nod2* KO mice and in the uninjured control small bowel (not shown). The *Nod2* KO mice showed an increased band at 40 kDa, corresponding to active MMP-2, and an increased band at 90 kDa, corresponding to active MMP-9. However, the bands at 60 kDa representing activity of both MMP-2 and MMP-9 were equally distributed between the WT and *Nod2* KO mice. This increase in enzyme activity corresponded to the increased gene expression measured by PCR.

were included in the analysis of the wellness score, weight course, and stool consistency. The wellness score (B) of the WT and *Nod2* KO mice was measured daily. A score of 11 represented maximal well-being, as seen in unoperated mice. Both groups recovered quickly after 24 hours. The weight course (C) showed similar weight loss during the experimental phase for the WT and *Nod2* KO mice, with a maximum loss during the initial 24 hours postoperation and plateauing after 72 hours. Results are expressed as percent weight compared to preoperative weight (% start). Stool consistency (D) changed toward a looser stool in both groups after bowel resection for 48 hours and normalized thereafter. The difference in stool consistency at day 1 postoperative was not significant. For A-D, n = 20 for the WT mice and n = 20 for the *Nod2* KO mice. Results for B, C, and D are expressed as median + interquartile ratio.

The data showed that *Nod2* deficiency led to a higher matrix turnover at the anastomosis, leading to a weaker anastomotic strength as measured by bursting pressure.

Histology and Immunohistochemistry

Hematoxylin and eosin staining showed equal formation of granulation tissue at the anastomosis in both groups. Cellular proliferation as measured by PCNA staining was slightly lower in the *Nod2* KO mice (represented in Fig. 5A). To show the specificity of the *Nod2* status, 2 key enzymes for wound healing—arginase I and inducible nitric oxide synthase (iNOS)—were investigated. The WT mice showed a very localized and structured arginase I and iNOS expression, whereas in the *Nod2* KO mice the expression was rather unorganized. Semi-quantitative histological analysis was performed in 4 anastomoses from each group. The independent and blinded observers closely agreed in their scoring, as indicated by a kappa of 0.5. Immunohistochemistry for iNOS showed significantly lower iNOS expression at the anastomosis in the *Nod2* KO mice (Fig. 5B), whereas arginase I expression was unchanged.

mRNA Expression of Transforming Growth Factor-ß, Tumor Necrosis Factor-α, Arginase I, and iNOS

The quantitative expression of 2 key cytokines involved in wound healing revealed a significantly increased expression of tumor necrosis factor-α and transforming growth factor-ß. Whereas iNOS expression was unchanged, arginase I expression was also increased in the *Nod2* KO mice (Fig. 6). Because arginase I and iNOS are normally expressed in a distinct timely manner in anastomotic healing, this finding suggested that the effect was specific and not only a general upregulation of inflammation.

DISCUSSION

The present data show that extended resection of the terminal ileum with primary end-to-end jejuno-colostomy is associated with impaired anastomotic healing in *Nod2* KO mice. Because *Nod2* KO mice do not develop inflammation of the gut per se, the effect is specific to the anastomosis.

We established this model involving the resection of 11 cm of the terminal ileum including the cecum because it led to a highly reproducible, compensated short-bowel syndrome as shown by the full recovery of the wellness score after 48 hours and the stabilization of weight loss during the experimental phase[18] and because it mimics an often encountered situation in patients with CD. Healing after this extensive resection is essential because failure often leads to type I short-bowel syndrome. Preoperative weight loss and malnutrition, especially hypoalbuminemia, impair healing in clinical and experimental conditions,[22, 23] but weight loss and the wellness score were equal in both groups of mice, ruling out the possibility that

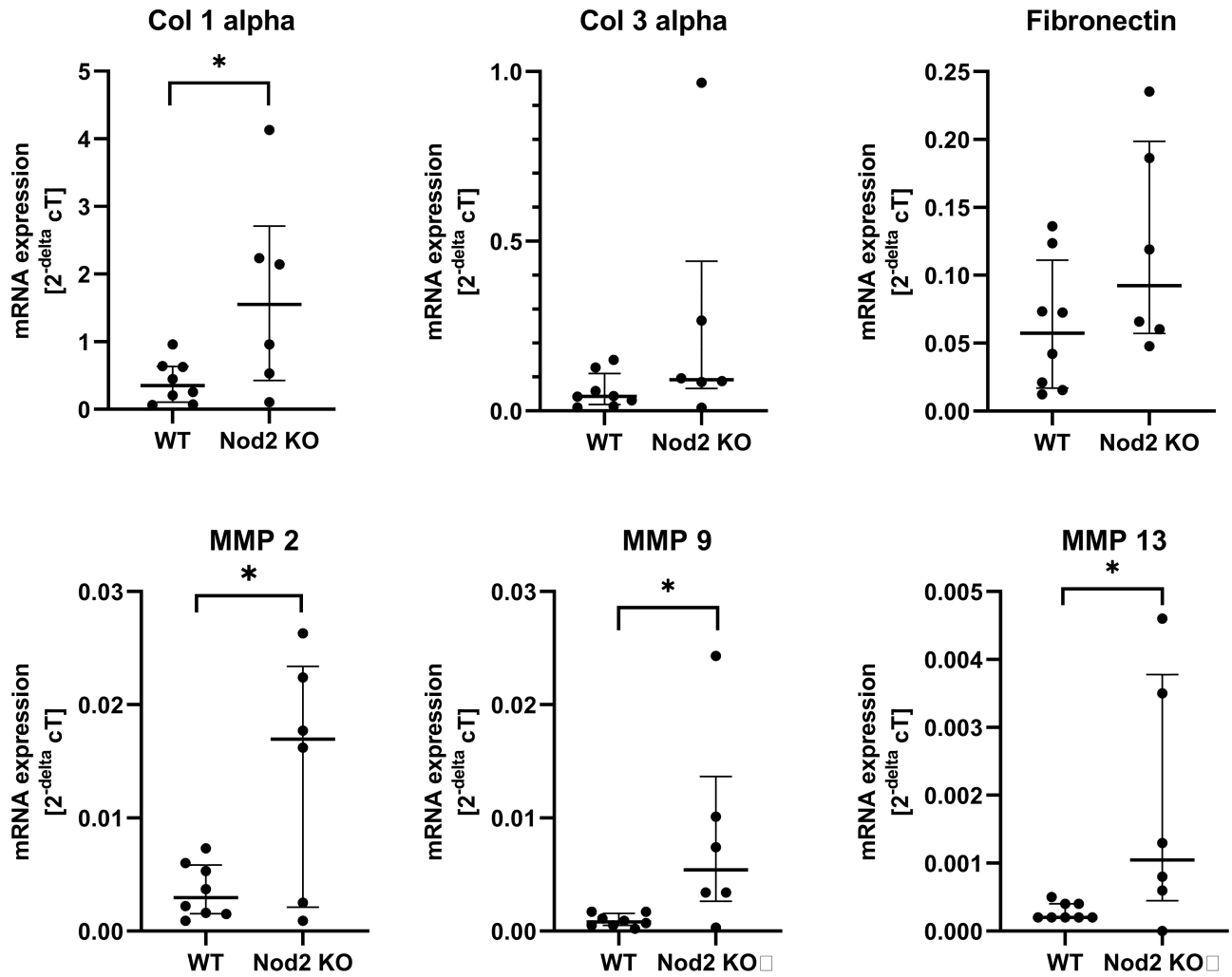

FIGURE 3. Results of the mRNA expression by quantitative real-time PCR and predesigned TaqMan gene expression assays (see Supplementary Table 1), which were normalized to the housekeeping gene *GAPDH*. Expression levels of the genes of interest are given as $2^{-\Delta cT}$. Surprisingly but constantly, expression was very homogeneous in the WT mice compared with a rather wide-ranging expression in the *Nod2* KO mice. Each dot represents the mean of 1 mouse, which was run in triplicate. The middle bar represents the median of the group + IQR. *$P < 0.05$ between groups. Col 1 indicates collagen 1; Col 3, collagen 3; IQR, interquartile ratio.

general postoperative deterioration caused impaired healing. Stool consistency was temporarily looser in the *Nod2* KO mice, suggesting that short-term postoperative adaptation may differ; however, previous work has shown that histomorphological adaptation is equal at days 7 and 14 postoperatively in both groups.[19]

Anastomotic healing is a well-orchestrated cascade of cellular and cell-mediated events. Systemic and local factors may affect this cascade, leading to impaired healing. Patients with *NOD2* mutations have worse clinical outcome in sepsis, CD, colitis, and other clinical conditions.[13, 24] Previous research has used *Nod2* KO mice as models to study the influence of NOD2 on immunological mechanisms. In general, *Nod2* KO mice are healthy, with normal leukocyte, lymphoid, and myeloid cell composition; normal intestines[25, 26]; and normal systemic response to a toxic challenge.[26] Our *Nod2* KO mice showed no obvious phenotypic alterations, and the numerically increased postoperative mortality could not be attributed to a specific cause.

Our data show for the first time that *Nod2* KO mice have weaker anastomoses than WT mice, as indicated by the decreased bursting pressure. However, we saw no difference in the leakage rate between both groups. The leakage rate in rodents is generally low because they form adhesions covering the anastomosis.[20] Therefore, leakage cannot be used as an outcome parameter as it is in humans. Instead, bursting pressure is the best way to assay the quality of the anastomosis. Bursting pressure is a functional parameter that cannot be directly correlated

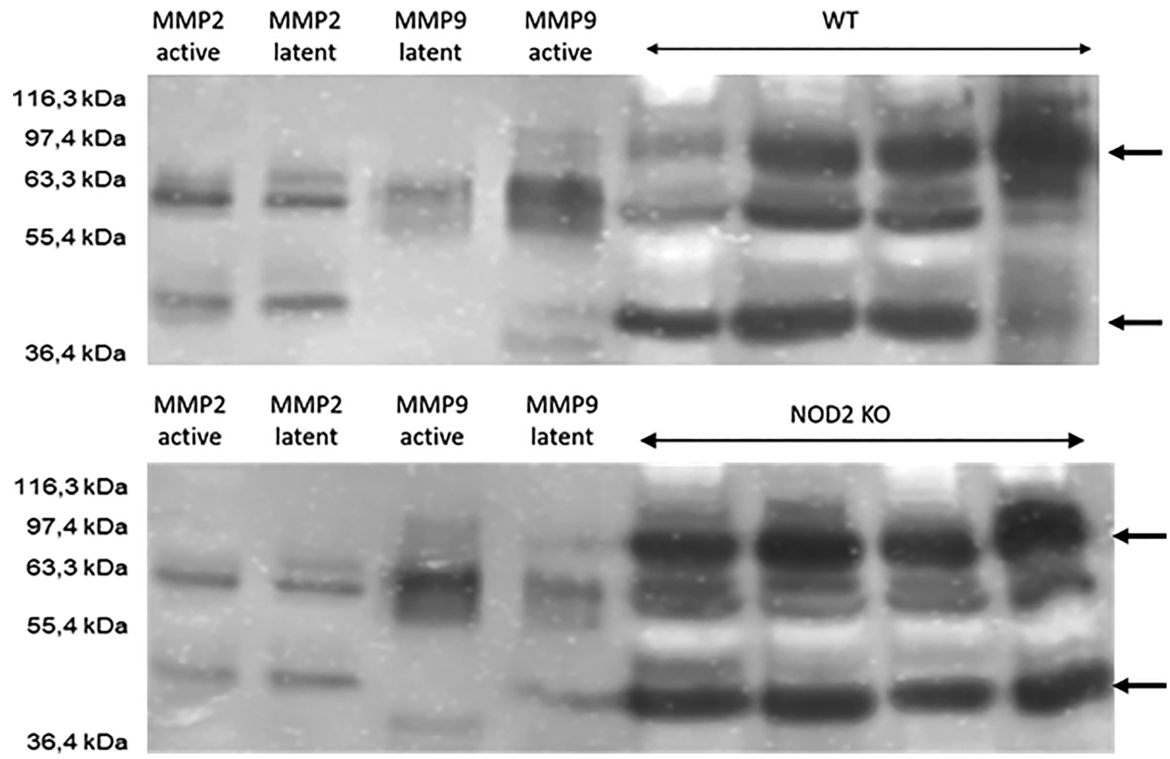

FIGURE 4. Zymography for the WT (upper panel) and *Nod2* KO mice (lower panel) using lysates from anastomotic tissue. Four probes per group were run and compared. The first 4 lanes show standards for active and latent MMP-2 and MMP-9. Unoperated small bowel of the WT and *Nod2* KO mice showed the same distribution pattern of MMPs, ruling out a difference in baseline expression between both groups (not shown). The arrows depicts MMP-2 and MMP-9 at 40 kDa and 90 kDa, respectively.

with collagen deposition as determined by OHP concentration.[27] Accordingly, the resulting OHP content and the amount of granulation tissue at the anastomosis were equal in both groups. Further, the significantly lower bursting pressure was not mediated by impaired collagen synthesis. Rather, matrix turnover was significantly increased in the *Nod2* KO mice as measured by collagen 1 gene expression and MMP-2, -9, and -13 gene expression along with enzyme activity measured in zymography. Regulation of MMP activity is central to anastomotic healing, as shown by the beneficial effects of MMP inhibition.[28]

The wide range of gene expression displayed in the *Nod2* KO mice and the histology of the anastomoses suggested that the orchestrated healing seen in the WT group and shown as a typical example in Fig. 5A was abandoned and that a more "chaotic" healing took place in the *Nod2* KO mice. This hypothesis was underlined by the immunohistochemistry for iNOS and arginase I, which normally occurs in a timely pattern in anastomotic healing[29] but appeared more diffuse in the *Nod2* KO anastomoses. This finding is in accordance with the results from excisional cutaneous wound healing in *Nod2*-deficient mice, where the macrophage phenotype changed to an inflammatory phenotype and wound healing was delayed.[15] The increased MMP-9 and MMP-13 expression seen in the *Nod2* KO mice could originate from a change to an inflammatory cell phenotype.[30] One mechanism of *NOD2* mutations in CD is the diminished downregulation of interleukin-12 signaling. This finding accounts for the observation that patients with CD with *NOD2* mutations have an increased NF-κB activation.[31] The *Nod2*-deficient mice also showed an enhanced T_H1 cytokine production, and macrophages from these mice displayed an increased Toll-like receptor 2–mediated activation of NF-κB.[32] This activation of the inflammatory pathway could explain the more chaotic histology and the increased tumor necrosis factor-α levels at the anastomosis seen in our model.

There are controversial data regarding whether *NOD2* deficiency alters the composition of intestinal bacteria per se.[33, 34] Previous work has shown that this model of ICR is accompanied by an altered gut microbiome.[19] We can therefore not rule out that this alteration influences anastomotic healing. An altered microbiome with persistent *Enterobacteriaceae* at the anastomosis has been suggested to be responsible for anastomotic leakage.[35] Furthermore, local *Enterococcus* may contribute to increased MMP-9 activity and therefore higher collagen degradation, leading to more frequent anastomotic leakage.[36] Although epithelial healing in CD involves defensins and patients with *NOD2* mutations have fewer α-defensins,[37] it

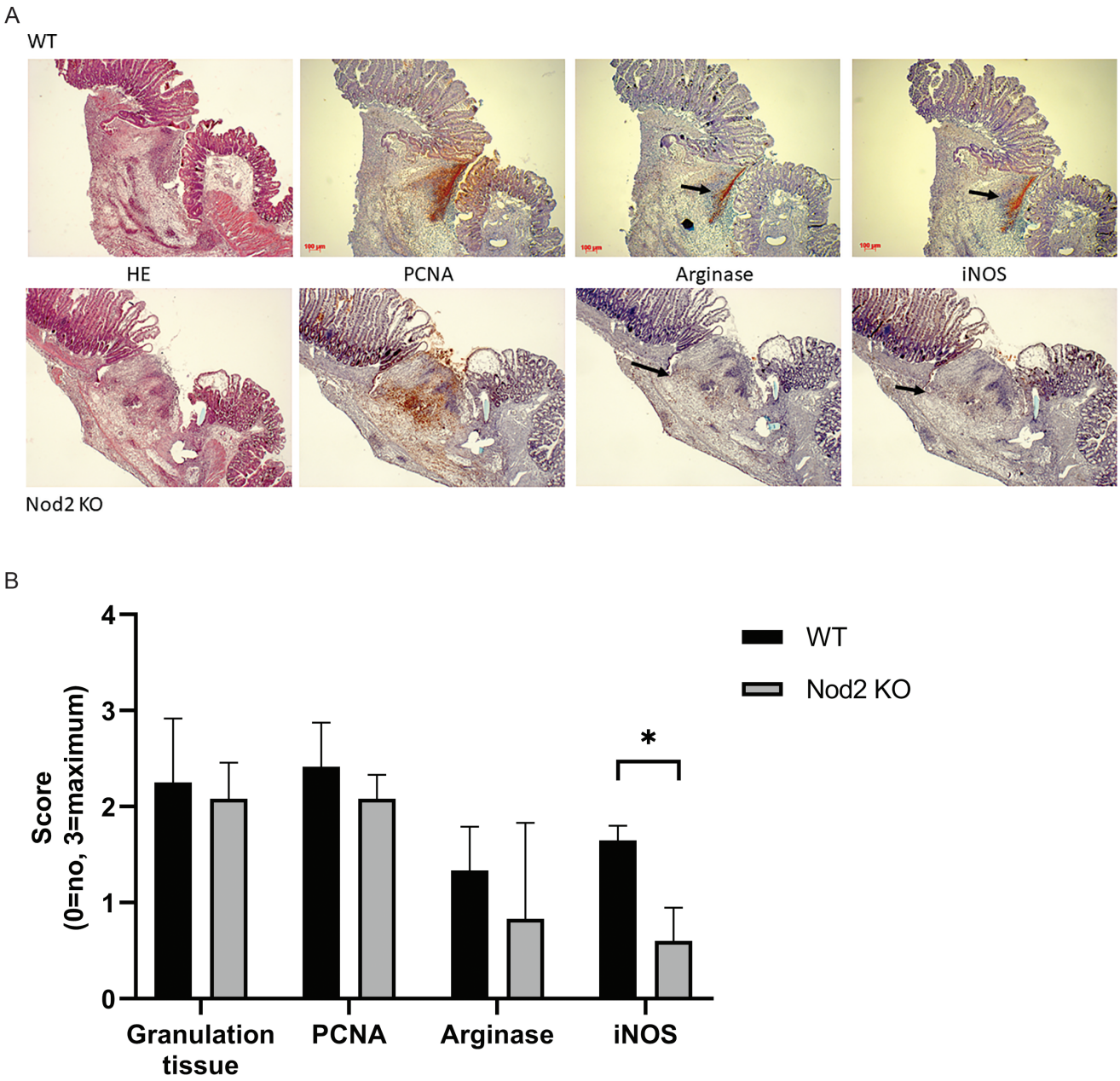

FIGURE 5. (5A), Representative picture of an anastomosis harvested on postoperative day 5 (10× magnification). The arrow indicates the zone of arginase I or iNOS expression in the WT mice (upper panel) and the *Nod2* KO mice (lower panel). (5B) Results of the semi-quantitative analysis of the histology. Sections of the anastomosis were analyzed in a blinded manner by 6 different individuals and scored as following: absence = 0, slight = 1, moderate = 2, and massive = 3. Granulation tissue formation as measured by HE staining ($P = 0.3$) and cell proliferation as measured by PCNA staining ($P = 0.069$) showed no significant difference between both groups. The iNOS expression, however, was significantly reduced at the anastomosis ($P < 0.05$; Mann-Whitney *U* test). The results are expressed as median + IQR, n = 4 per group. HE indicates hematoxylin and eosin; IQR, interquartile ratio.

is unknown whether full-thickness anastomotic healing is also influenced by local defensins. However, it is unlikely that the weaker anastomotic strength predominantly resulted from a NOD2-mediated reduced defensin secretion from the Paneth cells because we removed the entire terminal ileum and therefore the major Paneth cell pool in the control group as well in our model. We are currently investigating whether ICR is accompanied by a specific bacterial selection at the anastomosis in *Nod2* KO mice. Because current concepts of local antimicrobial decontamination are used to decrease the leakage rate, local antimicrobial decontamination could represent a therapeutic target for patients with *NOD2* mutations.[38]

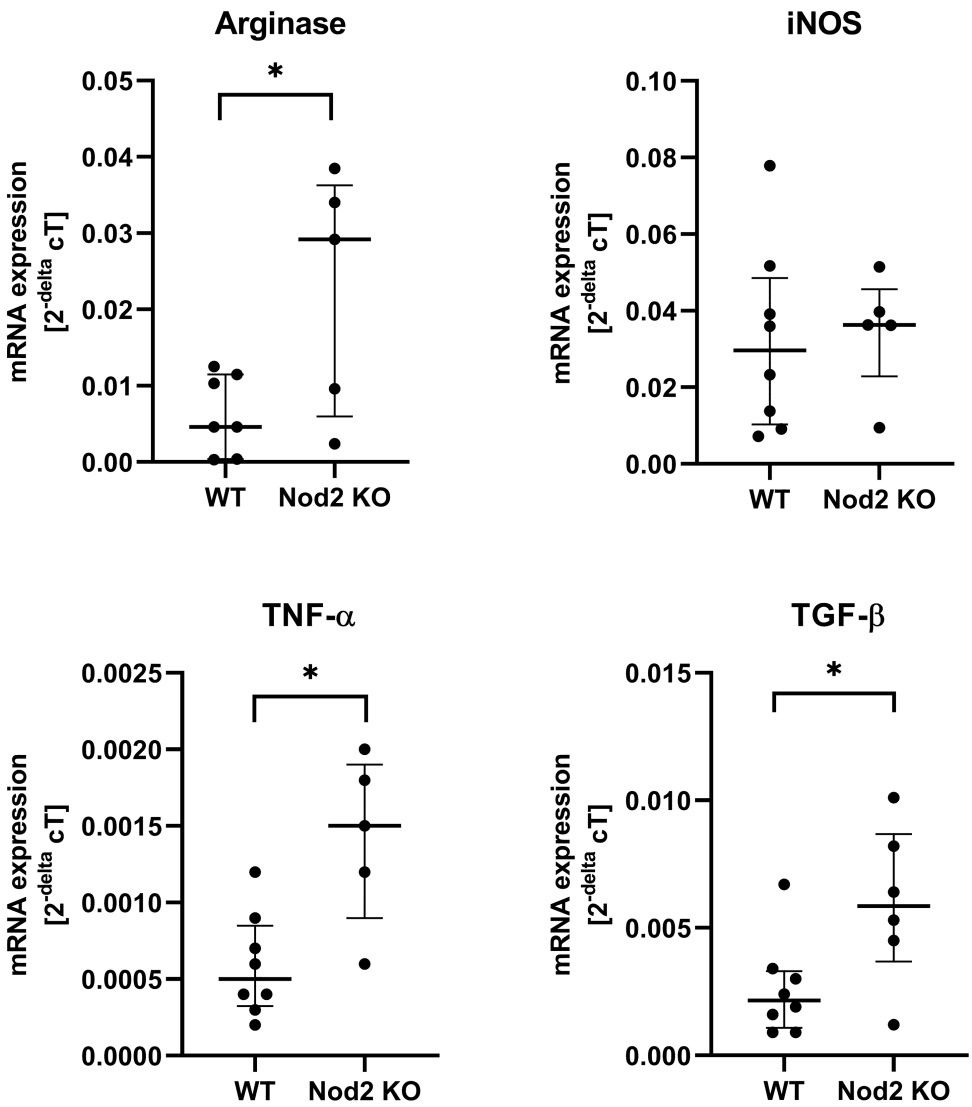

FIGURE 6. mRNA expression for key cytokines transforming growth factor-ß and tumor necrosis factor-α for wound healing and arginase I and iNOS are displayed. Each dot represents the result of 1 mouse, run in triplicate; the bar represents the median + IQR for each group. *$P < 0.05$ between groups, n = 5 to 8 per group. IQR indicates the interquartile ratio.

CONCLUSIONS

Herein, we show for the first time that gastrointestinal healing as shown by jejuno-colic anastomosis is impaired in *Nod2*-deficient mice after extended small-bowel resection. This finding could experimentally explain why some patients with CD and *NOD2* deficiency have a deleterious outcome after ICR in the clinical setting. Investigating patients with CD with failed anastomotic healing for *NOD2* mutations could be a first step toward further clarifying the role of *NOD2* mutations in clinical outcomes.

SUPPLEMENTARY DATA

Supplementary data are available at *Inflammatory Bowel Diseases* online.

REFERENCES

1. Frolkis AD, Dykeman J, Negrón ME, et al. Risk of surgery for inflammatory bowel diseases has decreased over time: a systematic review and meta-analysis of population-based studies. *Gastroenterology.* 2013;145:996–1006.
2. Ploug T, Andersen K, Hansen K, et al. Influence of adalimumab treatment on anastomotic strength, degree of inflammation, and collagen formation: an experimental study on the small intestine of rabbits. *Inflamm Bowel Dis.* 2013;19:254–258.
3. Papaconstantinou I, Zeglinas C, Gazouli M, et al. Effect of infliximab on the healing of intestinal anastomosis. An experimental study in rats. *Int J Surg.* 2014;12:969–975.
4. Fumery M, Seksik P, Auzolle C, et al.; REMIND study group investigators. Postoperative complications after ileocecal resection in Crohn's disease: a prospective study from the REMIND Group. *Am J Gastroenterol.* 2017;112:337–345.
5. Sidiq T, Yoshihama S, Downs I, et al. Nod2: a critical regulator of ileal microbiota and Crohn's disease. *Front Immunol.* 2016;7:367.
6. Connelly TM, Berg AS, Harris L 3rd, et al. Genetic determinants associated with early age of diagnosis of IBD. *Dis Colon Rectum.* 2015;58:321–327.
7. Naser SA, Arce M, Khaja A, et al. Role of ATG16L, NOD2 and IL23R in Crohn's disease pathogenesis. *World J Gastroenterol.* 2012;18:412–424.

8. Mendoza JL, Murillo LS, Fernández L, et al. Prevalence of mutations of the NOD2/CARD15 gene and relation to phenotype in Spanish patients with Crohn disease. *Scand J Gastroenterol.* 2003;38:1235–1240.
9. Rescigno M, Nieuwenhuis EE. The role of altered microbial signaling via mutant NODs in intestinal inflammation. *Curr Opin Gastroenterol.* 2007;23:21–26.
10. Nasir BF, Griffiths L, Nasir A, et al. Perianal disease combined with NOD2 genotype predicts need for IBD-related surgery in Crohn's disease patients from a population-based cohort. *J Clin Gastroenterol.* 2013;47:242–245.
11. Alvarez-Lobos M, Arostegui JI, Sans M, et al. Crohn's disease patients carrying Nod2/CARD15 gene variants have an increased and early need for first surgery due to stricturing disease and higher rate of surgical recurrence. *Ann Surg.* 2005;242:693–700.
12. Angelberger S, Reinisch W, Dejaco C, et al. NOD2/CARD15 gene variants are linked to failure of antibiotic treatment in perianal fistulating Crohn's disease. *Am J Gastroenterol.* 2008;103:1197–1202.
13. Brenmoehl J, Herfarth H, Glück T, et al. Genetic variants in the NOD2/CARD15 gene are associated with early mortality in sepsis patients. *Intensive Care Med.* 2007;33:1541–1548.
14. Schäffler H, Schneider N, Hsieh CJ, et al. NOD2 mutations are associated with the development of intestinal failure in the absence of Crohn's disease. *Clin Nutr.* 2013;32:1029–1035.
15. Campbell L, Williams H, Crompton RA, et al. Nod2 deficiency impairs inflammatory and epithelial aspects of the cutaneous wound-healing response. *J Pathol.* 2013;229:121–131.
16. Williams H, Crompton RA, Thomason HA, et al. Cutaneous Nod2 expression regulates the skin microbiome and wound healing in a murine model. *J Invest Dermatol.* 2017;137:2427–2436.
17. Williams H, Campbell L, Crompton RA, et al. Microbial host interactions and impaired wound healing in mice and humans: defining a role for BD14 and NOD2. *J Invest Dermatol.* 2018;138:2264–2274.
18. Berlin P, Reiner J, Wobar J, et al. Villus growth, increased intestinal epithelial sodium selectivity, and hyperaldosteronism are mechanisms of adaptation in a murine model of short bowel syndrome. *Dig Dis Sci.* 2019;64:1158–1170.
19. Berlin P, Reiner J, Witte M, et al. Nod2 deficiency functionally impairs adaptation to short bowel syndrome via alterations of the epithelial barrier function. *Am J Physiol Gastrointest Liver Physiol.* 2019;317:G727–G738.
20. Komen N, van der Wal HC, Ditzel M, et al. Colorectal anastomotic leakage: a new experimental model. *J Surg Res.* 2009;155:7–12.
21. Radulescu A, Zhang HY, Chen CL, et al. Heparin-binding EGF-like growth factor promotes intestinal anastomotic healing. *J Surg Res.* 2011;171:540–550.
22. Nisar PJ, Appau KA, Remzi FH, et al. Preoperative hypoalbuminemia is associated with adverse outcomes after ileoanal pouch surgery. *Inflamm Bowel Dis.* 2012;18:1034–1041.
23. Galata C, Kienle P, Weiss C, et al. Risk factors for early postoperative complications in patients with Crohn's disease after colorectal surgery other than ileocecal resection or right hemicolectomy. *Int J Colorectal Dis.* 2019;34:293–300.
24. Brant SR, Picco MF, Achkar JP, et al. Defining complex contributions of NOD2/CARD15 gene mutations, age at onset, and tobacco use on Crohn's disease phenotypes. *Inflamm Bowel Dis.* 2003;9:281–289.
25. Kobayashi KS, Chamaillard M, Ogura Y, et al. Nod2-dependent regulation of innate and adaptive immunity in the intestinal tract. *Science.* 2005;307:731–734.
26. Stroo I, Butter LM, Claessen N, et al. Phenotyping of Nod1/2 double deficient mice and characterization of Nod1/2 in systemic inflammation and associated renal disease. *Biol Open.* 2012;1:1239–1247.
27. Hendriks T, Mastboom WJ. Healing of experimental intestinal anastomoses. Parameters for repair. *Dis Colon Rectum.* 1990;33:891–901.
28. Ågren MS, Andersen TL, Andersen L, et al. Nonselective matrix metalloproteinase but not tumor necrosis factor-α inhibition effectively preserves the early critical colon anastomotic integrity. *Int J Colorectal Dis.* 2011;26:329–337.
29. Witte MB, Vogt N, Stuelten C, et al. Arginase acts as an alternative pathway of L-arginine metabolism in experimental colon anastomosis. *J Gastrointest Surg.* 2003;7:378–385.
30. Verhofstad MH, Lomme RM, de Man BM, et al. Intestinal anastomoses from diabetic rats contain supranormal levels of gelatinase activity. *Dis Colon Rectum.* 2002;45:554–561.
31. Strober W, Murray PJ, Kitani A, et al. Signalling pathways and molecular interactions of NOD1 and NOD2. *Nat Rev Immunol.* 2006;6:9–20.
32. Watanabe T, Kitani A, Murray PJ, et al. NOD2 is a negative regulator of Toll-like receptor 2-mediated T helper type 1 responses. *Nat Immunol.* 2004;5:800–808.
33. Robertson SJ, Zhou JY, Geddes K, et al. Nod1 and Nod2 signaling does not alter the composition of intestinal bacterial communities at homeostasis. *Gut Microbes.* 2013;4:222–231.
34. Rehman A, Sina C, Gavrilova O, et al. Nod2 is essential for temporal development of intestinal microbial communities. *Gut.* 2011;60:1354–1362.
35. Gaines S, Shao C, Hyman N, et al. Gut microbiome influences on anastomotic leak and recurrence rates following colorectal cancer surgery. *Br J Surg.* 2018;105:e131–e141.
36. Shogan BD, Belogortseva N, Luong PM, et al. Collagen degradation and MMP9 activation by *Enterococcus faecalis* contribute to intestinal anastomotic leak. *Sci Transl Med.* 2015;7:286ra68.
37. Wehkamp J, Harder J, Weichenthal M, et al. NOD2 (CARD15) mutations in Crohn's disease are associated with diminished mucosal alpha-defensin expression. *Gut.* 2004;53:1658–1664.
38. Abis GSA, Stockmann HBAC, Bonjer HJ, et al.; SELECT trial study group. Randomized clinical trial of selective decontamination of the digestive tract in elective colorectal cancer surgery (SELECT trial). *Br J Surg.* 2019;106:355–363.